WiFi-RTT Indoor Positioning

Christian Gentner, Markus Ulmschneider, Isabel Kuehner, Armin Dammann
German Aerospace Center (DLR)
Institute of Communications and Navigation
Oberpfaffenhofen, 82234 Wessling, Germany
Email: {Christian.Gentner, Markus.Ulmschneider, Isabel.Kuehner, Armin.Dammann}@dlr.de

***Abstract*—Global navigation satellite systems (GNSSs) can deliver very good position estimates under optimum conditions. However, especially in urban and indoor scenarios with severe multipath propagation and blocking of satellites by buildings the accuracy loss can be very large. Using WiFi for indoor positioning is a common approach because WiFi infrastructure is widely deployed. Recently the WiFi IEEE 802.11-2016 standard was released, which includes a fine timing measurement (FTM) protocol, more commonly known as WiFi-round-trip-time (WiFi-RTT) protocol, for WiFi ranging. This paper researches timing based positioning algorithms, in this case using WiFi-RTT distance estimates. Based on two measurement campaigns, in an antenna measurement chamber and in a typical indoor environment, a WiFi-RTT distance error model is derived. Both measurement campaigns show, that the distance is underestimated, hence, the estimated distance is lower than the true distance. The WiFi-RTT distance error model is included in the likelihood function of a particle filter (PF) and the positioning performances is evaluated in an indoor scenario. These evaluations show clearly the possibility of using WiFi-RTT distance estimates for indoor positioning.**

I. Introduction

The proliferation of smartphones has made positioning technologies available to a wide range of users [1]. For outdoor localization, global navigation satellite systems (GNSSs) are the most well-known and mostly used technologies for positioning. In open sky conditions, GNSSs provide sufficient position accuracy for most mass market applications. However, inside buildings or in urban canyons the GNSS positioning accuracy might be drastically reduced. In these situations, the GNSS signals might be affected by multipath effects, received with low power or even blocked. To enhance the positioning performance, different methods and sensor systems can provide position information to complement GNSSs [2], [3]. Most of the indoor positioning systems use local infrastructure like positioning with radio frequency identification (RFID) [4], mobile communication base-stations [5], [6], Bluetooth, WiFi [7] or ultra-wideband (UWB) systems [8]–[13].

Using WiFi for indoor positioning is a common approach because WiFi infrastructure is widely deployed [14], [15]. Fingerprinting approaches for positioning with WiFi are very common. They measure the received signal strengths (RSSs) of signals coming from nearby WiFi transmitters. Fingerprinting approaches consist typically of a training phase and a positioning phase: In the training phase, RSSs measurements are recorded and stored at defined locations in order to build a RSSs map of the environment. During the positioning phase, the position of the receiver can be estimated by correlating the measured RSS with the preconstructed map. The coordinates corresponding to the closest RSS match are returned as an estimate for the receiver position. The main drawback of the fingerprinting approach is that the generation and maintenance of the RSSs maps is time-consuming and expensive when performed over wide areas. Additionally, the RSS can vary extremely caused by body shading, changes in the environment, different receiver hardware, etc. Hence, it is very hard to obtain an accurate position estimate based on this type of measurements.

In 2016 a new WiFi standard was released which promises a great improvement in the positioning accuracy. The IEEE 802.11-2016 standard, sometimes referred to as IEEE 802.11mc, includes a fine timing measurement (FTM) protocol for WiFi ranging [16]. The WiFi FTM protocol, more commonly known as WiFi-round-trip-time (WiFi-RTT) protocol allows computing devices, e.g. smartphones, to estimate the distance to nearby WiFi access points (APs). The devices do not have to be connected to the APs. The distance is calculated on the device, which helps to maintain privacy. The ranging process starts at the device with a standard WiFi scan and the device sends a FTM request to the AP for estimating the WiFi-RTT. If the AP accepts the FTM request, the device and the AP are exchanging messages where the arrival and departure time stamps of the messages on both sides are recorded. At the end, the time stamps recorded at the AP are sent to the device which can calculate the total WiFi-RTT.

In 2018, Google released with Android Pie a smartphone operating system supporting WiFi FTM. Hence, WiFi FTM became available to a wide range of developers, especially for indoor scenarios. First researches are evaluating the IEEE 802.11-2016 standard, see e.g. [17]–[20]. The authors of [17], [20], [21] are analyzing the round-trip-time (RTT) ranging accuracy in different environments and with different devices. In [18], [19] first positioning examples were shown using a smartphone.

This paper evaluates the WiFi-RTT protocol using a Google Pixel 3 and Google WiFi APs. We can show clearly the benefits of using WiFi-RTT distance estimates for positioning. The WiFi-RTT distance estimation accuracy depends on the used hardware and also on the signal propagation conditions. Especially indoors, where WiFi-RTT will mostly be used, the signal might be blocked, degraded by multipath effects or received with low power. Hence, the WiFi-RTT measurements

978-1-7281-0244-3/20/$31.00 ©2020 IEEE

are expected to be noisy and biased. In order to cope with the noisy and biased distance estimates, it is essential to model the WiFi-RTT distance estimation errors. To see the WiFi-RTT distance estimation accuracy without the influence of multipath propagation and signal blockage, we evaluated the WiFi-RTT distance estimation in an antenna measurement chamber where multipath propagation is suppressed. Similar to [17], the WiFi-RTT distance estimates are underestimated and we obtain RTT distance estimations which are lower than the true distance. In a second measurement campaign, in an indoor environment, we obtain similar WiFi-RTT distance estimation errors. Based on the indoor measurements, we model the WiFi-RTT distance estimation error by a Gaussian mixture model. This error model is evaluated on measurements in the same indoor environment, where we use the WiFi-RTT distance error model in the likelihood function of a particle filter (PF).

The paper is structured as follows. In Section II, we introduce briefly the WiFi FTM protocol of the IEEE 802.11-2016 standard. Section III evaluates the WiFi-RTT distance estimates based on two measurement campaigns: in an antenna measurement chamber and in an indoor environment; additionally, we derive a WiFi-RTT distance estimation error model. Afterwards, the positioning performance is evaluated in Section IV. Finally, Section V concludes the paper.

II. WiFi FTM protocol

The IEEE 802.11-2016 standardizes a FTM protocol that enables a pair of WiFi devices to estimate the distance between them. The FTM protocol contains five messages, two are sent by the initiating device, e.g. a smartphone, and two by the responding device, e.g. an AP. Fig. 1 shows the details for the FTM protocol, where a mobile device initiates the FTM process by sending a FTM request to an AP. An AP that supports the FTM protocol, responds to the FTM request either to agree or refuse the ranging process. In the case of agreement, the AP starts to send a FTM message and waits for its acknowledgement (ACK) and transmits afterwards the FTM result. The propagation delay between the mobile device and the i-th AP can be estimated by

$$z_i(t_k) = c \cdot \frac{(\tau_{4,i}(t_k) - \tau_{1,i}(t_k)) - (\tau_{3,i}(t_k) - \tau_{2,i}(t_k))}{2}, \quad (1)$$

based on the transmitting timestamp of the FTM message and the reception timestamp of its ACK, illustrated in Fig. 1. c denotes the speed of light. The AP may send multiple FTM messages in a burst for averaging the estimated distances, see e.g. [17]–[21] for more details.

III. WiFi-RTT measurements

A. Measurements in an antenna measurement chamber

In order to see the accuracy of the FTM protocol, we performed measurements in an antenna measurement chamber as shown in Fig. 2. Usually multipath propagation and non-line-of-sight (NLoS) biases the range estimates. In the antenna measurement chamber, multipath propagation is kept to a minimum and only the line-of-sight (LoS) propagation path should be present.

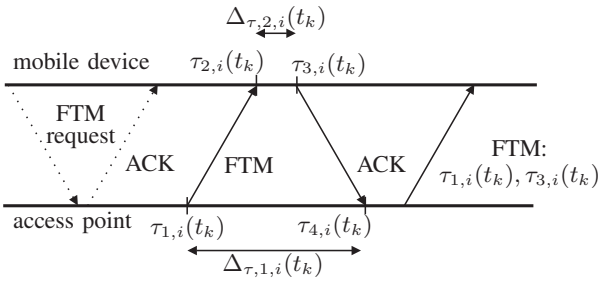

Fig. 1: Overview of the WiFi FTM protocol: a mobile device measures its distance to an AP.

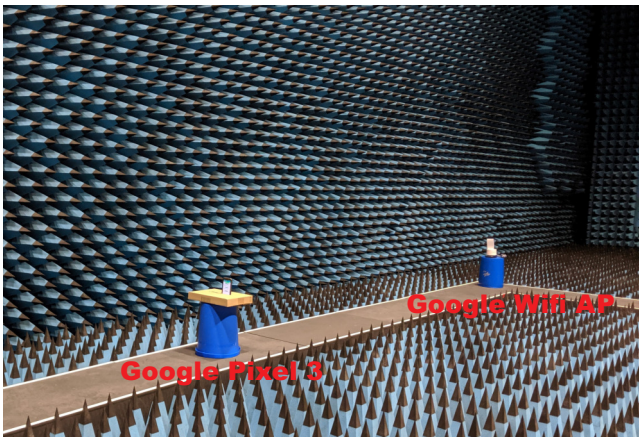

Fig. 2: Measurement campaign in an antenna measurement chamber.

First, we analyze the WiFi-RTT distance estimation for the Google Pixel 3 in texting mode, shown in Fig. 2. We recorded continuously the WiFi-RTT distance estimates for different distances between the Google Pixel 3 and the Google WiFi APs. Fig. 7 shows the WiFi-RTT distance estimates as a function of the true distance in meter. The black dashed line indicates the true values. We can observe that the system underestimates the WiFi-RTT distances with about $-1.3\,\mathrm{m}$. This is also visible if we look on the distribution of the WiFi-RTT distance estimation errors, shown in Fig. 4 by the blue line. The underestimated WiFi-RTT distances could be caused by internal calibration of the WiFi devices or multipath compensation algorithms that process the measurements in the firmware.

To see the influence of the 3D-location of the Google Pixel 3 on the WiFi-RTT distance estimates, we positioned the Google Pixel 3 on different positions and rotation angles. Fig. 5 shows the WiFi-RTT distance estimation errors for different turning angles. The Google Pixel 3 was turned clockwise in steps of $22.5°$. At $0°$ the Google Pixel 3 was facing in the direction of the AP. Fig. 5a shows the WiFi-RTT distance estimation errors for the Google Pixel 3 in texting mode. In Fig. 5b the display is facing up and Fig. 5c the display is facing down. The WiFi-RTT distance estimation errors are similar to Fig. 7

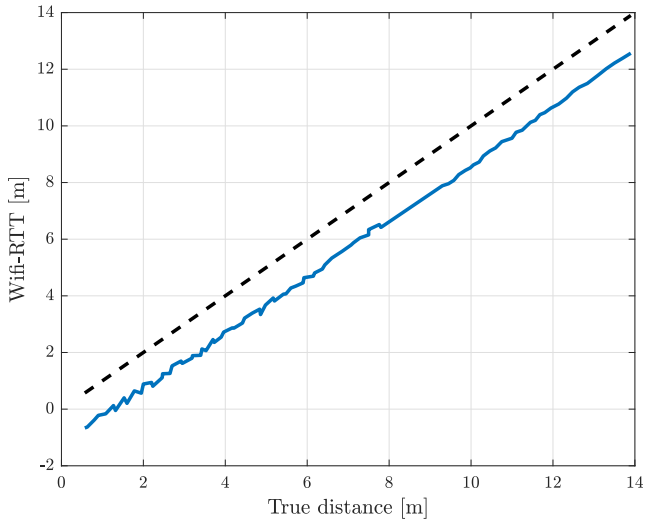

Fig. 3: Estimated WiFi-RTT distance in meter as a function of the true distance, shown in blue. The black dashed line indicates the true values.

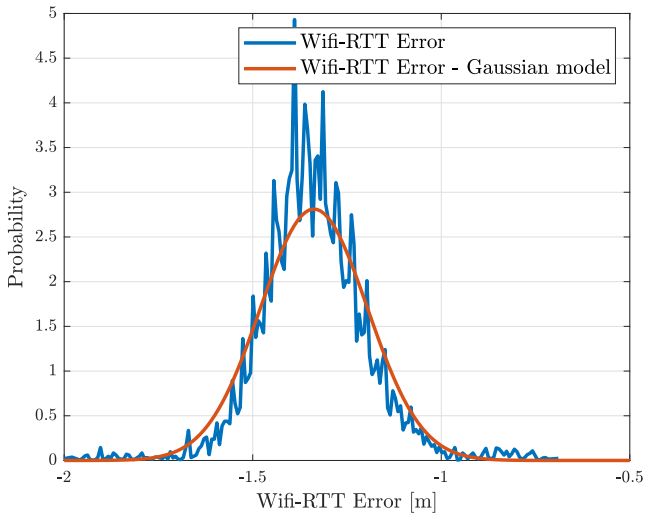

Fig. 4: Distribution of the WiFi-RTT distance estimation errors in blue. The red line indicates the single Gaussian model.

and Fig. 4, hence, the distances are underestimated in all different positions also with a mean of $\mu = -1.3\,\mathrm{m}$. Even if we get an underestimated distance of $-1.3\,\mathrm{m}$, the WiFi-RTT distance estimation does not depend on the 3D-location of the Google Pixel 3. In order to see the WiFi-RTT distance estimates in multipath environments, we performed additional measurements in an indoor environment, see Section III-B.

B. Measurements in an indoor environment

To see the WiFi-RTT distance estimation performance in a multipath environment an indoor measurement campaign was performed using the Google Pixel 3 smartphone and six Google WiFi APs. Fig. 6 shows the indoor measurement scenario in top view with six Google WiFi AP positions indicated by APi for $i = 1, \ldots, 6$. The Google Pixel 3 was

TABLE I: Statistical parameters of the Gaussian WiFi-RTT distance estimation error model of (2).

k	p_k	μ_k	σ_k^2
1	0.22	$0.1795[m]$	$1.3017[m^2]$
2	0.78	$-0.9503[m]$	$0.2055[m^2]$

mounted on a robot which was moving in the area indicated in gray in Fig. 6. A Vicon motion capture system was used to obtain the position of the Google Pixel 3. The Vicon motion capture system is capable to track the motion of the Google Pixel 3 in the measurement room with an accuracy of less than $1\,\mathrm{cm}$. Four Google WiFi APs, AP2 - AP5, were placed in the same room with the Google Pixel 3. During the robot movement, the LoS path between the Google WiFi AP2-AP5 and the Google Pixel 3 is most of the time present, however sometimes shaded by furniture. The other two Google WiFi APs, AP1 and AP6, were placed in the corridor.

Fig. 7 shows the WiFi-RTT distance estimates as a function of the true distances between the Google Pixel 3 and the different APs. Equivalently to the measurements in the antenna measurement chamber, described in Section III-A, the system underestimates the distances. If we use additionally the calibration mean error of the antenna measurement chamber $\mu = -1.3\,\mathrm{m}$ as a prior knowledge, we obtain the gray lines in Fig. 7. We can observe, that the WiFi-RTT distance estimates are more accurate if $\mu = -1.3\,\mathrm{m}$ is added. Fig. 8 shows in blue the distribution of the WiFi-RTT distance estimation errors. We can see that the distribution has still a Gaussian shape and has a negative mean value, however, $\mu \neq -1.3\,\mathrm{m}$.

In order to use the WiFi-RTT distance estimates for positioning, we have to model the WiFi-RTT distance estimation errors. As mentioned before, the distribution of Fig. 8 shows similarity with a Gaussian distribution, but has a larger tail than a typical Gaussian distribution. One way to model a non-Gaussian probability density function (PDF) is using a Gaussian mixture model (GMM). A GMM of order K (GMM(K)) is defined as the sum of weighted Gaussian distributions with

$$f(x) = \sum_{k=1}^{K} p_k \mathcal{N}(\mu_k, \sigma_k) \quad \text{with} \quad \sum_{k=1}^{K} p_k = 1, \qquad (2)$$

where $\mathcal{N}(\mu_k, \sigma_k)$ represents a Gaussian distribution with mean μ_k and standard deviation σ_k, weighted by p_k for $k = 1, ..., K$. In general, a GMM can asymptotically represent an arbitrary shaped PDF. To construct a Gaussian mixture model, we used the Akaike information criterion (AIC) and Bayesian information criterion (BIC) to define the number of necessary Gaussians. Both criteria show, that a Gaussian mixture of two should be used for this model with the parameters shown in Table I and indicated in Fig. 8 by the red line. The dotted lines in Fig. 8 indicate the two individual Gaussian distributions. The model is different than the model obtained in the antenna measurement chamber, however, it includes also effects of multipath propagation and signal blockage.

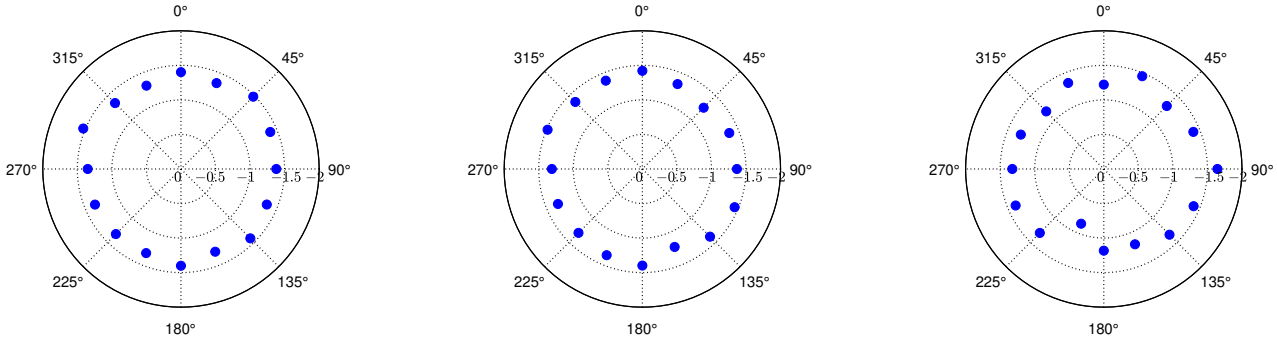

(a) Google Pixel 3 - texting mode (b) Google Pixel 3 - display facing up (c) Google Pixel 3 - display facing down

Fig. 5: WiFi-RTT distance estimation errors for different mobile positions and rotation angles.

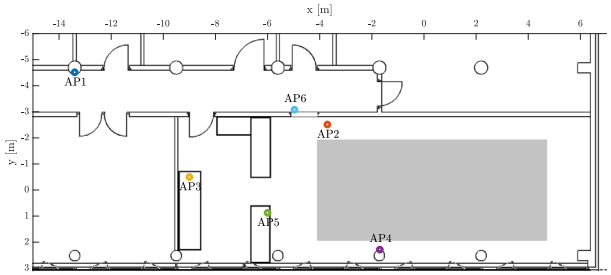

Fig. 6: Indoor measurement environment: The Google Pixel 3 was mounted on a robot which was driving in the area marked in gray; 6 Google WiFi APs were mounted.

IV. Positioning Example using WiFi-RTT

In order to see the positioning performance using the derived WiFi-RTT distance error model of Section III-B, we performed three different measurements: robot only; robot and moving persons; moving person. Details can be found in Table II. Fig. 9 shows the indoor measurement scenario in top view with the six AP positions indicated by APi for $i = 1, \ldots, 6$ and the robot track in red and the person track in blue.

TABLE II: Three different indoor measurements.

Robot - only	The robot is moving in the room carrying the Google Pixel 3 in texting mode. The red line in Fig. 9 shows the ground truth of the robot movement.
Robot - moving persons	The robot is moving in the room carrying the Google Pixel 3 in texting mode. The red line in Fig. 9 shows the ground truth of the robot movement. Additionally, people are moving around in the room who are influencing the signal propagation by attenuation, blockage or diffraction.
Person	A person is caring the Google Pixel 3 in texting mode. The blue line in Fig. 9 shows the ground truth of the movement of the person.

Algorithm 1: Sequential importance resampling (SIR) PF

$\{\mathbf{x}^{(j)}(t_k), w^{(j)}(t_k)\}_{j=1}^{N_p} =$
SIR $\left(\{\mathbf{x}^{(j)}(t_{k-1}), w^{(j)}(t_{k-1})\}_{j=1}^{N_p}, \mathbf{z}(t_k)\right)$

for $j = 1 : N_p$ **do**
  Draw: $\mathbf{x}^{(j)}(t_k) \sim \mathsf{p}\big(\mathbf{x}^{(j)}(t_k)|\mathbf{x}^{(j)}(t_{k-1})\big)$;
  Calculate: $w^{*(j)}(t_k) = \mathsf{p}\big(\mathbf{z}(t_k)|\mathbf{x}^{(j)}(t_k)\big)$;
Calculate: $W(t_k) = \sum_{j=1}^{N_p} w^{*(j)}(t_k)$;
for $j = 1 : N_p$ **do**
  Normalize: $w^{(j)}(t_k) = \frac{w^{*(j)}(t_k)}{W(t_k)}$;
Resample see [22]: Obtaining $\{\mathbf{x}^{(j)}(t_k), w^{(j)}(t_k)\}_{j=1}^{N_s}$;

The positioning filter is implemented by a SIR PF, see [22]–[24]. PFs are based on sequential Monte Carlo methods which implement recursive Bayesian filters by Monte Carlo integration [22], [25]. PFs approximate the probability density of the state vector $\mathbf{x}(t_k)$ at time step t_k by N_p particles with the particle state vector $\mathbf{x}^{(j)}(t_k)$ and the normalized weight $w^{(j)}(t_k)$. Algorithm 1 shows a pseudo-code of the SIR PF. From Algorithm 1, we can see that two models have to be implemented for the SIR PF in order to be used: a state transition model calculating the transitional prior $\mathsf{p}\big(\mathbf{x}(t_k)|\mathbf{x}(t_{k-1})\big)$ and the measurement model calculating the likelihood $\mathsf{p}\big(\mathbf{z}(t_k)|\mathbf{x}(t_k)\big)$, where $\mathbf{z}(t_k) = \big[z_1(t_k), \ldots, z_{N(t_k)}(t_k)\big]^T$ denotes the WiFi-RTT distance estimates for $i = 1, \ldots, N(t_k)$ APs at time step t_k. These two models represent the two major blocks of any sequential Bayesian filter implementation. We use $N_p = 3000$ particles and a standard random walk transition model. In the likelihood $\mathsf{p}\big(\mathbf{z}(t_k)|\mathbf{x}(t_k)\big)$ we use the obtained WiFi-RTT distance error model. Hence, we obtain for the j-th particle

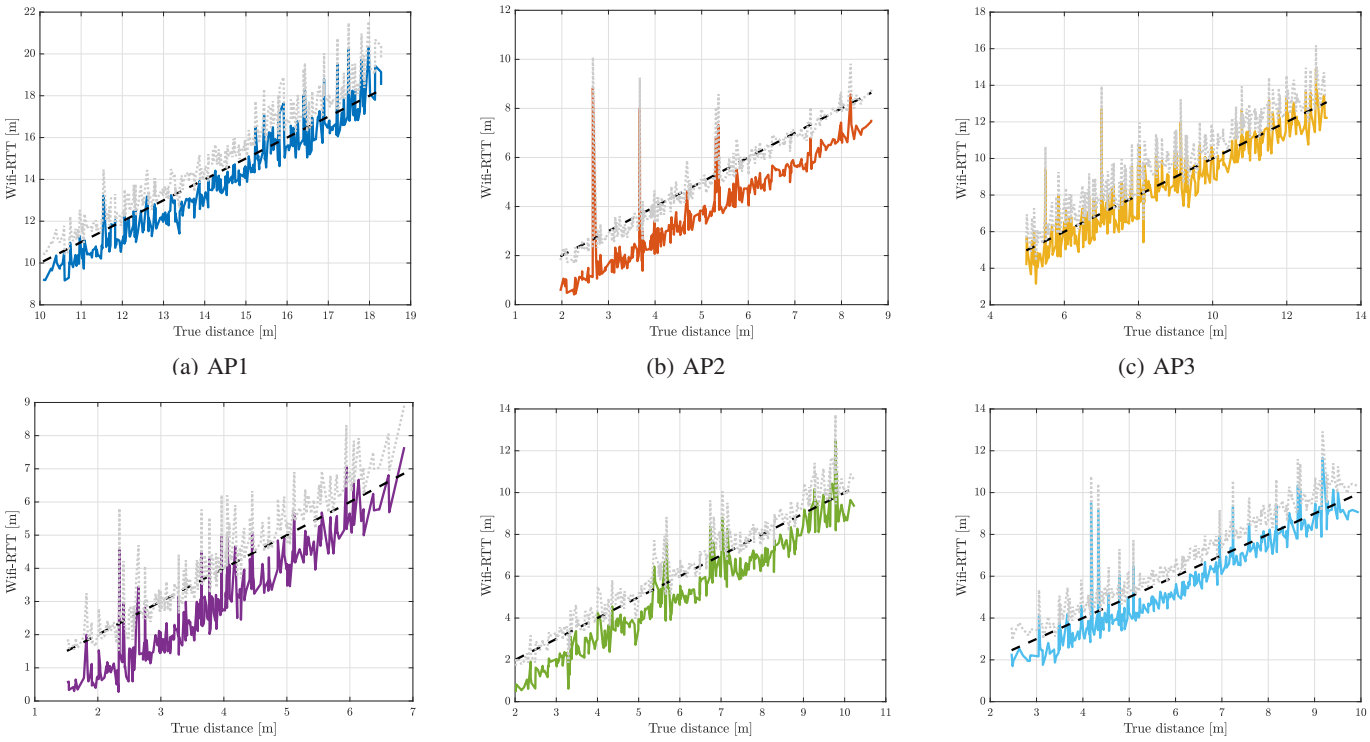

(a) AP1 (b) AP2 (c) AP3

(d) AP4 (e) AP5 (f) AP6

Fig. 7: Estimated WiFi-RTT distance in meter as a function of the true distance for all APs. The black dashed line indicates the true values. If the calibration mean error of the antenna measurement chamber $\mu = -1.3\,\mathrm{m}$ is used as a prior knowledge, the gray lines are obtained.

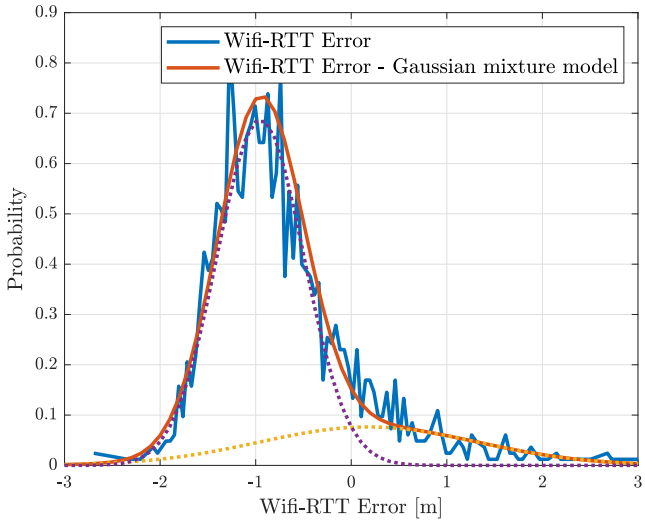

Fig. 8: Distribution of the WiFi-RTT distance estimation errors for all APs. The blue line indicates the distribution of the WiFi-RTT distance estimation errors, the red line indicates the Gaussian mixture model.

$$\mathrm{p}\big(\mathbf{z}(t_k)|\mathbf{x}^{(j)}(t_k)\big) = \prod_{i=1}^{N(t_k)} \sum_{k=1}^{2} p_k \, \frac{1}{\sqrt{2\pi}\sigma_k} \, e^{-\frac{(z_i(t_k)-\mu_k-d_i^{(j)}(t_k))^2}{2\sigma^2}}, \qquad (3)$$

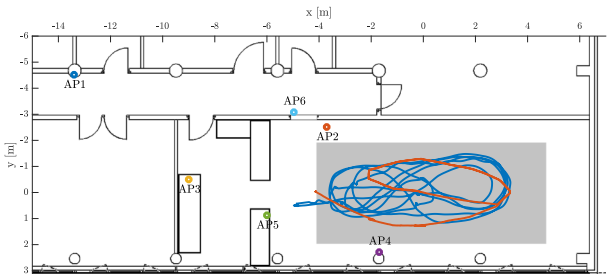

Fig. 9: Indoor measurement scenarios, where we performed three different measurements: robot only (red line); robot and moving persons (red line); moving person (blue line) - see Table II for details.

with the mean μ_k and standard deviation σ_k of Table I and

$$d_i^{(j)}(t_k) = \|\mathbf{x}^{(j)}(t_k) - \mathbf{x}_{\mathrm{AP},i}\|\,, \qquad (4)$$

where $\mathbf{x}_{\mathrm{AP},i}$ denotes the i-th AP position. Because the PF includes randomness, the position estimates differ for each evaluation due to a finite number of particles even if the same measurement data are used. Therefore, we perform 100 independent evaluations based on the same measurement data.

Even if the Google Pixel 3 offers many senor data, the evaluations use only the WiFi-RTT distance estimates. This allows to see the positioning performance only based on WiFi-

TABLE III: Mean μ and standard deviation σ of the absolute positioning error.

	μ /σ
Robot - only: proposed model	0.47 / 0.27
Robot - only: standard model	1.07 / 0.34
Robot - moving persons: proposed model	0.54 / 0.35
Robot - moving persons: standard model	0.96 / 0.43
Person: proposed model	0.93 / 0.88
Person: standard model	1.38 / 0.95

RTT distance estimates. In a real indoor environment, the density of WiFi APs might not be that dense, hence, other sensors of the smartphone should be fused to obtain a stable position solution. This will be a focus for future research.

Fig. 10 shows the cumulative distribution functions (CDFs) of the positioning error for the three different measurements using the PF with a standard Gaussian measurement model (dashed lines) and with the proposed Gaussian mixture measurement model (solid lines). First, we can observe that we can obtain an accurate position estimate for all measurements. Especially for the proposed WiFi-RTT distance error model we obtain for the robot in 92 percent of the cases an error below $1\,\mathrm{m}$ even if persons are moving around. In the case of the moving person, we obtain an error below $1\,\mathrm{m}$ in 70 percent of the cases. When a person is walking with the Google Pixel 3 in texting mode, the distance estimates are also affected by shadowing of the signal by the human body. Finally, Table III summarizes the mean and standard deviation of the positioning errors. Please note, the recording application running on the Google Pixel 3 is re-scanning the WiFi network every 15 s for 5 s. In these 5 s, the Google Pixel 3 can not use the WiFi FTM protocol and can not estimate the distance to the nearby APs. Hence, in these 5 s, the particles are only propagated based on the transition model. Future research, should use in these situations other sensors of the Google Pixel 3 to obtain better position estimates.

V. Conclusions

This paper studies and implements a positioning approach using the IEEE 802.11-2016 standard. The standard includes a fine timing measurement (FTM) protocol for WiFi ranging. The WiFi FTM protocol, more commonly known as WiFi-round-trip-time (WiFi-RTT) protocol allows to estimate the distance between two WiFi devices. For our studies, we use the Google Pixel 3 and Google WiFi access points (APs). First, we evaluate the WiFi-RTT distance estimates in an antenna measurement chamber where multipath propagation should be suppressed. The results show that the round-trip-time (RTT) distance estimates are lower than the true distance by a mean of $-1.3\,\mathrm{m}$. Equivalent results are obtained in an indoor environment. To obtain better positioning results, a WiFi-RTT distance error model is derived based on the WiFi-RTT distance errors of the measurements in the indoor environment.

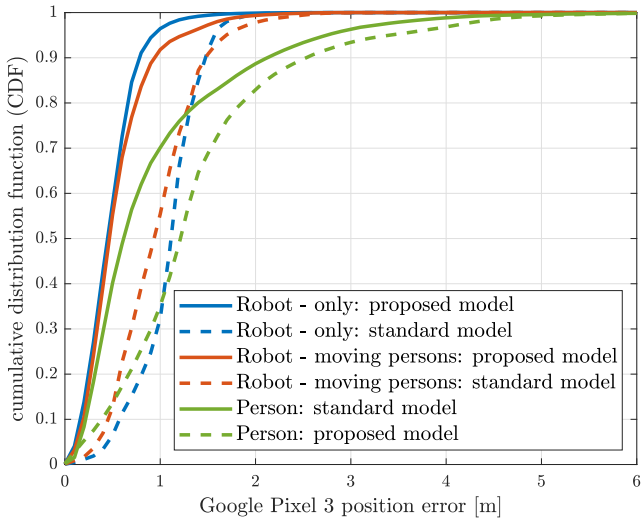

Fig. 10: CDFs of the Google Pixel 3 positioning error for the proposed (solid lines) and a standard measurement model (dashed lines).

For the WiFi-RTT distance error model a Gaussian mixture model of two is derived and included in the likelihood function of a particle filter (PF).

References

[1] G. Seco-Granados, J. López-Salcedo, D. Jiménez-Baños, and G. López-Risueño, "Challenges in Indoor Global Navigation Satellite Systems," *IEEE Signal Process. Mag.*, vol. 29, no. 2, pp. 108–131, Mar. 2012.

[2] H. Liu, H. Darabi, P. Banerjee, and J. Liu, "Survey of Wireless Indoor Positioning Techniques and Systems," *IEEE Trans. Syst., Man, Cybern. C*, vol. 37, no. 6, pp. 1067–1080, Nov. 2007.

[3] D. Dardari, P. Closas, and P. M. Djuric, "Indoor Tracking: Theory, Methods, and Technologies," *IEEE Trans. Veh. Technol.*, vol. 64, no. 4, pp. 1263–1278, Apr. 2015.

[4] "Performance-Based Evaluation of RFID-based Indoor Location Sensing Solutions for the Built Environment," *Adv. Eng. Inf.*, vol. 25, no. 3, pp. 535 – 546, Aug. 2011.

[5] A. H. Sayed, A. Tarighat, and N. Khajehnouri, "Network-Based Wireless Location: Challenges Faced in Developing Techniques for Accurate Wireless Location Information," *IEEE Signal Process. Mag.*, vol. 22, pp. 24–40, Jul. 2005.

[6] Y. Zhao, "Standardization of Mobile Phone Positioning for 3G Systems," *IEEE Commun. Mag.*, vol. 40, no. 7, pp. 108–116, Jul. 2002.

[7] K. Kaemarungsi and P. Krishnamurthy, "Properties of Indoor Received Signal Strength for WLAN Location Fingerprinting," Aug. 2004, pp. 14–23.

[8] M. Win and R. Scholtz, "Characterization of Ultra-Wide Bandwidth Wireless Indoor Channels: a Communication-Theoretic View," *IEEE J. Sel. Areas Commun.*, vol. 20, no. 9, pp. 1613–1627, Dec. 2002.

[9] A. Molisch, D. Cassioli, C.-C. Chong, S. Emami, A. Fort, B. Kannan, J. Karedal, J. Kunisch, H. Schantz, K. Siwiak, and M. Win, "A Comprehensive Standardized Model for Ultrawideband Propagation Channels," *IEEE Trans. Antennas Propag.*, vol. 54, no. 11, pp. 3151–3166, Nov. 2006.

[10] C. Steiner and A. Wittneben, "Low Complexity Location Fingerprinting With Generalized UWB Energy Detection Receivers," *IEEE Trans. Signal Process.*, vol. 58, no. 3, pp. 1756–1767, Mar. 2010.

[11] I. Oppermann, M. Hämäläinen, and J. Iinatti, *UWB: Theory and Applications*. John Wiley & Sons, 2005.

[12] C. Gentner and M. Ulmschneider, "Simultaneous Localization and Mapping for Pedestrians using Low-Cost Ultra-Wideband System and Gyroscope," Saporo, Japan, Sep. 2017.

[13] R. Karásek and C. Gentner, "Stochastic Data Association for Multipath Assisted Positioning Using a Single Transmitter," *IEEE Access*, vol. 8, 2020.
[14] Y. Luo, O. Hoeber, and Y. Chen, "Enhancing WiFi Fingerprinting for Indoor Positioning using Human-Centric Collaborative Feedback," *Human-centric Computing and Inf. Sciences*, vol. 3, no. 1, p. 2, 2013.
[15] P. Bahl and V. N. Padmanabhan, "RADAR: an In-Building RF-Based User Location and Tracking System," in *Proc. IEEE Conf. on Comp. Commun. (INFOCOM)*, vol. 2, 2000, pp. 775–784 vol.2.
[16] "IEEE Standard for Information technologyTelecommunications and information exchange between systems Local and metropolitan area networksSpecific requirements - Part 11: Wireless LAN Medium Access Control (MAC) and Physical Layer (PHY) Specifications," *IEEE Std 802.11-2016 (Revision of IEEE Std 802.11-2012)*, pp. 1–3534, Dec 2016.
[17] M. Ibrahim, H. Liu, M. Jawahar, V. Nguyen, M. Gruteser, R. Howard, B. Yu, and F. Bai, "Verification: Accuracy evaluation of WiFi fine time measurements on an open platform," in *Proceedings of the 24th Annual International Conference on Mobile Computing and Networking*, 2018, pp. 417–427.
[18] K. Han, S. M. Yu, and S. Kim, "Smartphone-based Indoor Localization Using Wi-Fi Fine Timing Measurement," in *2019 International Conference on Indoor Positioning and Indoor Navigation (IPIN)*, Sep. 2019, pp. 1–5.
[19] G. Guo, R. Chen, F. Ye, X. Peng, Z. Liu, and Y. Pan, "Indoor Smartphone Localization: A Hybrid WiFi RTT-RSS Ranging Approach," *IEEE Access*, vol. 7, pp. 176 767–176 781, 2019.
[20] N. Dvorecki, O. Bar-Shalom, L. Banin, and Y. Amizur, "A Machine Learning Approach for Wi-Fi RTT Ranging," 01 2019.
[21] L. Banin, U. Schatzberg, and Y. Amizur, "WiFi FTM and map information fusion for accurate positioning," in *2016 International Conference on Indoor Positioning and Indoor Navigation (IPIN)*, 2016.
[22] M. Arulampalam, S. Maskell, N. Gordon, and T. Clapp, "A Tutorial on Particle Filters for Online Nonlinear/Non-Gaussian Bayesian Tracking," *IEEE Trans. Signal Process.*, vol. 50, no. 2, pp. 174–188, Feb. 2002.
[23] C. Gentner, S. Zhang, and T. Jost, "Log-PF: Particle Filtering in Logarithm Domain," *Journal of Electrical and Computer Engineering*, vol. 2018, Jan. 2018.
[24] C. Gentner, T. Jost, W. Wang, S. Zhang, A. Dammann, and U.-C. Fiebig, "Multipath Assisted Positioning with Simultaneous Localization and Mapping," *IEEE Trans. Wireless Commun.*, vol. 15, no. 9, pp. 6104–6117, Sep. 2016.
[25] N. Gordon, D. Salmond, and A. F. M. Smith, "Novel Approach to Nonlinear/Non-Gaussian Bayesian State Estimation," *IEE Proc. Radar Signal Processing*, vol. 140, no. 2, pp. 107–113, 1993.